Modern radio engineering and telecommunication systems

Современные радиотехнические и телекоммуникационные системы

UDC 621.396.946
https://doi.org/10.32362/2500-316X-2025-13-1-89-102
EDN OVSTWY

CC BY

RESEARCH ARTICLE

Modeling of digital spatial processing under conditions of troposphere propagation of centimeter radio waves for wireless telecommunication

Ilia W. Peshkov [1, @], Dmitry N. Borisov [2]

[1] *Bunin Yelets State University, Yelets, 399770 Russia*
[2] *Voronezh State University, Voronezh, 394018 Russia*
[@] *Corresponding author, e-mail: ilvpeshkov@gmail.com*

Abstract

Objectives. A radio beam traveling through the layers of the atmosphere depends on the refractive index and its vertical variation. In this regard, attenuation may occur when radio rays propagate in a waveguide manner at low altitudes. A multipath fading effect may also occur when several rays reflected from different layers of the troposphere and having different spatial coordinates in elevation arrive at the receiver. The aim of the study is to simulate the operational algorithms of digital antenna arrays (DAA) in order to increase the range and reliability of radio communication using a tropospheric waveguide. The main advantage of the DAA consists in the high gain and controllability of the pattern shape. In order to evaluate algorithms for direction-of-arrival estimation with super-resolution and beamforming, it is necessary to select an appropriate method for modeling beam propagation in the layers of the troposphere. It is proposed to use DAA to increase the range and reliability of radio communications using a tropospheric waveguide. The performance of algorithms for direction-of-arrival estimation and beamforming in the troposphere can be evaluated using ray tracing simulation.

Methods. Parabolic equations are used to estimate the path losses of radio waves in the centimeter range. A ray tracing algorithm referring to a tropospheric waveguide is used to estimate the phases in the aperture of the receiving array. A spatial correlation matrix is reliably generated to form the basis for calculating coordinates using a super-resolution multiple signal classification (MUSIC) method and the weighting factor vector (algorithm for maximizing the signal-to-noise + noise ratio).

Results. Typical cases of a tropospheric waveguide based on a modified refractive index were considered. The bit error rate curves are obtained as a function of the geometry of the antenna arrays after the signal has passed through the tropospheric waveguide. Circular and spherical antenna arrays composed of directional antenna elements are considered.

Conclusions. Numerical studies suggest that the range of communication links using digital antenna arrays increases in the centimeter band. The best geometry for this purpose is circular, since providing the lowest bit error rate for binary phase-shift keyed signals.

Keywords: digital antenna array, direction-of-arrival estimation, MUSIC method, beamforming, tropospheric waveguide, simulation

© I.W. Peshkov, D.N. Borisov, 2025

• **Submitted:** 09.10.2023 • **Revised:** 22.07.2024 • **Accepted:** 10.12.2024

For citation: Peshkov I.W., Borisov D.N. Modeling of digital spatial processing under conditions of troposphere propagation of centimeter radio waves for wireless telecommunication. *Russian Technological Journal*. 2025;13(1):89–102. https://doi.org/10.32362/2500-316X-2025-13-1-89-102, https://elibrary.ru/OVSTWY

Financial disclosure: The authors have no financial or proprietary interest in any material or method mentioned.

The authors declare no conflicts of interest.

НАУЧНАЯ СТАТЬЯ

Моделирование цифровой пространственной обработки в условиях тропосферного распространения сантиметровых радиоволн для задач телекоммуникации

И.В. Пешков [1, @], **Д.Н. Борисов** [2]

[1] *Елецкий государственный университет им. И.А. Бунина, Елец, 399770 Россия*
[2] *Воронежский государственный университет, Воронеж, 394018 Россия*
[@] *Автор для переписки, e-mail: ilvpeshkov@gmail.com*

Резюме

Цели. Прохождение радиолуча в слоях атмосферы зависит от показателя преломления и характера его вертикального изменения. В связи с этим могут возникнуть условия, когда радиолучи на малых высотах будут распространяться волноводным образом. При этом происходит затухание сигнала с отличающимися угловыми координатами по углу места. Целью работы является исследование на основе моделирования алгоритмов работы цифровых антенных решеток (ЦАР) для повышения дальности и надежности радиосвязи в условиях тропосферного волновода. Основными преимуществами ЦАР являются высокий коэффициент усиления и управляемость формы диаграммы направленности. При этом необходимо воспользоваться методами моделирования распространения луча в слоях тропосферы для оценки работы алгоритмов оценки угловых координат со сверхразрешением с последующим диаграммообразованием.

Методы. В работе используется аппарат параболических уравнений для оценки коэффициента затуханий радиоволн сантиметрового диапазона, а также алгоритм трассировки лучей через тропосферный волновод для оценки фаз в раскрыве антенн ЦАР. В этом случае будет достоверно сформирована пространственная корреляционная матрица, являющаяся основой для вычисления координат со сверхразрешением (метод MUSIC) и вектора весовых коэффициентов (алгоритм максимизации отношения сигнал/помеха + шум).

Результаты. Рассмотрены типичные случаи возникновения тропосферного волновода на основе модифицированного показателя преломления. Получены графики вероятности битовых ошибок после прохождения сигнала по тропосферному волноводу при разной геометрии антенных решеток. Рассмотрены кольцевые и сферические решетки из направленных антенных элементов.

Выводы. Проведенные численные исследования позволяют сделать вывод, что дальность связи в диапазоне сантиметровых волн увеличивается с помощью ЦАР. Кроме того, установлено, что кольцевая антенная решетка позволяет получить самые низкие значения вероятности битовой ошибки при приеме дискретных радиосигналов в тропосферном волноводе.

Ключевые слова: цифровые антенные решетки, пеленгация, MUSIC, диаграммообразование, тропосферная связь, моделирование

• **Поступила:** 09.10.2023 • **Доработана:** 22.07.2024 • **Принята к опубликованию:** 10.12.2024

Для цитирования: Пешков И.В., Борисов Д.Н. Моделирование цифровой пространственной обработки в условиях тропосферного распространения сантиметровых радиоволн для задач телекоммуникации. *Russian Technological Journal*. 2025;13(1):89–102. https://doi.org/10.32362/2500-316X-2025-13-1-89-102, https://elibrary.ru/OVSTWY

Прозрачность финансовой деятельности: Авторы не имеют финансовой заинтересованности в представленных материалах или методах.

Авторы заявляют об отсутствии конфликта интересов.

INTRODUCTION

The propagation of ultrashort radio waves in the atmosphere is not typically rectilinear, but curved in such a way that the radio wave can undergo refraction in the lower layers and/or multiple reflections from the Earth's surface [1]. In this case, signals of centimeter wavelengths can reach receivers several hundred kilometers away from the transmitter [2–4]. This effect is due to temperature, humidity, and pressure differences in the layers of the troposphere, for which reason it has been named *tropospheric waveguide* [5–7]. This type of long-distance communication can be promising as it does not require expensive means such as satellites [8]. However, communication reliability and stability depends on factors such as the degree of attenuation, the accuracy of determining the height of the tropospheric waveguide in relation to the distance to the receiver, etc. [9]. In this regard, it is necessary to study the application of a digital beam-steering antenna array in tropospheric waveguide conditions as a means of overcoming the associated communication problems. Such devices allow digital shaping of the array pattern peaks and zeros in the desired directions.

The present work proposes a combined simulation method based on the stepwise determination of the loss value and phases of the centimeter range rays propagating in atmospheric layers as a function of the refractive index at different altitudes. The possibility of using digital antenna arrays (DAAs) for such communication is additionally investigated. The first step of the simulation consists in estimating the attenuation of the radio signal. Next, the propagation path from the transmitter to the receiving DAA is calculated using the ray tracing algorithm. Finally, the beamforming algorithms (estimation of the angular coordinates of all beams and digital formation of the array pattern) are modeled to calculate of the bit error rate (BER).

BEAM PROPAGATION IN THE TROPOSPHERE

It is known that the propagation path of a single ray is governed by the well-known Snell's law for a continuous spherically layered medium, as follows[1]:

$$n(h)(R_E + h)\cos e = \text{const}, \quad (1)$$

where n is the refractive index of the medium, h is the height above the Earth's surface, and R_E is the Earth's radius. For a more detailed consideration of the formation mechanism for tropospheric propagation, e represents the angle of the beam location.

The real part of the refractive index can be expressed as a function of atmospheric pressure, humidity, and air temperature. The formula for the index is semi-empirical and can be expressed as follows[2]:

$$n = 1 + 77.6 \cdot 10^{-6} \frac{P}{T} + 0.373 \frac{p}{T^2}, \quad (2)$$

where P is the atmospheric pressure in millibars; T is the temperature in degrees Kelvin; p is the water vapor pressure in millibars.

Equation (2) is known as the Debye formula. It has been shown to have an error of ±0.5% [10]. The refractive index n rarely exceeds 1.0004 at the surface. This introduces the so-called radio wave refraction N, which is defined as follows[3]:

$$N = (n-1) \cdot 10^6. \quad (3)$$

The propagation of radio waves depends more on refraction gradients than on N itself [10]. Typically, noticeable refraction gradients in the horizontal direction occur on much larger scales (tens of meters to tens of kilometers) than in the vertical direction (tens of meters to hundreds of meters). Therefore, the atmosphere is often assumed to be horizontally stratified, and only the height dependence of the refraction is considered, neglecting any horizontal variations.

[1] Recommendation ITU-R P.834-6. *Effects of tropospheric refraction on radiowave propagation* (in Russ.).
[2] The Handbook on Radiometeorology. ITU, 2014. https://www.itu.int/dms_pub/itu-r/opb/hdb/R-HDB-26-2013-OAS-PDF-R.pdf. Accessed October 09, 2023.
[3] Recommendation ITU-R P.453-12(09/2016). *Radio wave refraction index: its formula and refraction data* (in Russ.).

Similarly, the modified or changed refraction M is determined from the modified or changed index of refraction m to include the curvature of the Earth [11]:

$$M = (m-1)\cdot 10^6 = 10^6 \times \left(n - 1 + \frac{h}{R_E}\right) = \\ = N + 10^6 \cdot \frac{h}{R_E}. \quad (4)$$

Figure 1 depicts a simulation of the surface and elevated waveguides using a three-line curve referred to as a profile. The case shown in Fig. 1a illustrates the structure of a simple surface channel. Here, the waveguide extends from a certain boundary height to the Earth's surface, while the trapping layer, where the condition $dM/dh < 0$ favors wave refraction, extends along the entire wave propagation path. The *S*-shaped channel at the surface is shown in Fig. 1b. The trapping layer does not reach the surface since the condition $dM/dh > 0$ applies near the surface. In both cases, the depth of the channel is the height difference between the surface and the top of the channel where the minimum of the modified refraction profile is reached[4]. The general conditions for an elevated channel are summarized in Fig 1c, where the value of M at the Earth's surface is less than at the top of the channel, for which reason the channel cannot reach the surface.

As mentioned above, the appearance of the waveguide is the result of strong vertical changes in atmospheric refractive index between air masses of different temperature and humidity, especially at lower atmospheric levels. In this way, the tropospheric waveguide allows electromagnetic energy to propagate over long distances, enabling long-range radio communications over the horizon.

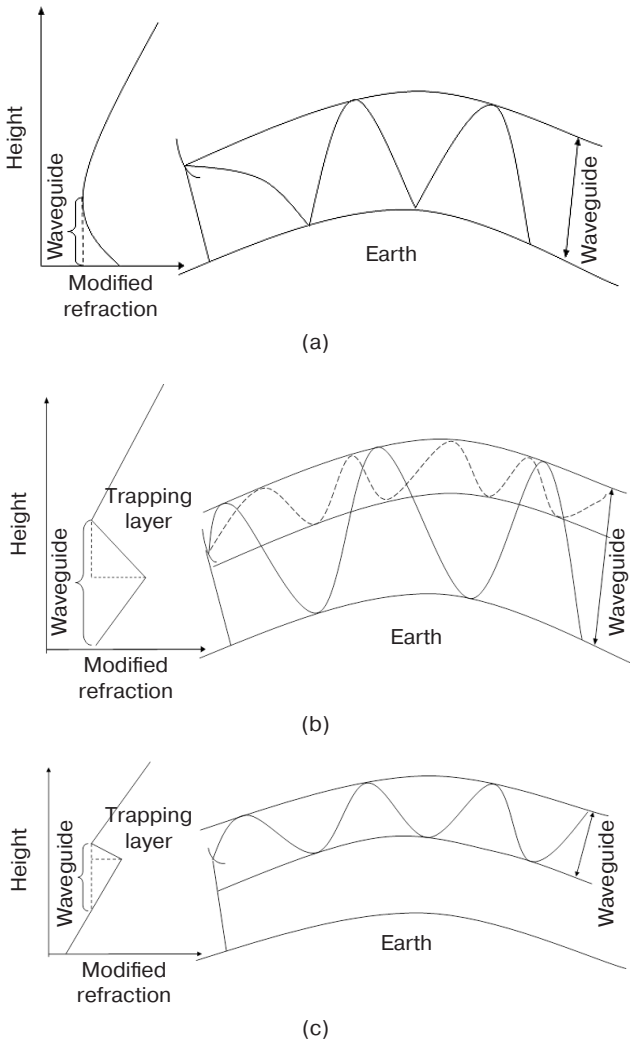

Fig. 1. *M*-profile for different conduction types: (a) simple surface (ground) waveguide, (b) surface waveguide, and (c) elevated waveguide

CALCULATION OF RADIO SIGNAL ATTENUATION USING THE PARABOLIC EQUATION METHOD

This section describes the parabolic equation (PE) apparatus for tropospheric radio propagation problems to estimate the degree of attenuation. Since its original introduction by Leontovich and Fock in 1946 [12], its design has been gradually improved.

According to the Helmholtz equation, the component φ of the electric or magnetic field satisfies the condition [13]:

$$\frac{\partial^2 \varphi}{\partial x^2} + \frac{\partial^2 \varphi}{\partial z^2} + k^2 n^2 \varphi = 0, \quad (5)$$

where k is the free space wave number and φ is the electromagnetic field component, either *Ey* or *Hy* for horizontal and vertical polarization, respectively.

We introduce the so-called reduced field function $u(x, z)$ as a function of the coordinates x and z:

$$\dot{u}(x,z) = e^{-ikx}\varphi(x,z). \quad (6)$$

The point of making this substitution and solving for $\dot{u}(x,z)$ instead of $\varphi(x, z)$ is that $\dot{u}(x,z)$ changes slowly depending on the propagation direction. Following this substitution, the scalar wave Eq. (5) takes the following form:

$$\left\{\frac{\partial^2}{\partial x^2} + \frac{\partial^2}{\partial z^2} + 2ik\frac{\partial}{\partial x} + k^2\left[n^2 - 1\right]\right\}\dot{u}(x,z) = 0. \quad (7)$$

[4] Lindquist T. *Wave Propagation Models in the Troposphere for Long-Range UHF/SHF Radio Connections.* PhD Thesis. 2020. https://urn.kb.se/resolve?urn=urn:nbn:se:kau:diva-80679. Accessed October 09, 2023.

Since this equation is still classified as elliptic rather than parabolic, it is acceptable to introduce a pseudo-differential operator $Q = \sqrt{\frac{1}{k^2}\frac{\partial^2}{\partial z^2} + n^2} = \sqrt{1+q}$, $q = \frac{1}{k^2}\frac{\partial^2}{\partial z^2} + (n(x,z)-1)$ and to factorize Eq. (7). This substitution makes the derivation more general [14]:

$$\left\{\frac{\partial}{\partial x} + ik\left(1-Q\right)\right\}\left\{\frac{\partial}{\partial x} + ik\left(1+Q\right)\right\}u = 0. \quad (8)$$

Equation (9) is simply repeated in steps of Δx until a target point with coordinates x, z is reached, provided that the initial reduced field $u(0, z)$ is known [12, 13]:

$$u\left(x+\Delta x, z\right) = \mathrm{e}^{ik\Delta x(Q-1)}u\left(x,z\right). \quad (9)$$

There are several methods for solving Eq. (9) [14]. The most widely referred to in the existing literature are the split-step Fourier PU, finite element, and finite difference methods[5].

After the field strength has been calculated in accordance with (9), it is necessary to estimate the degree of attenuation along the path by means of propagation and loss factors. The propagation factor *PF* (dB) is defined as the square of the ratio of the electric field amplitude at a given point under specified conditions to that of the same point under free propagation. Equation (10), which expresses the *PF* through the field relative to free space, also shows the relationship with the value of the propagation loss *PL* (dB) [15–17]:

$$PF = 20\lg\left|\dot{u}(x,z)\right| + 10\lg(r) + 10\lg(\lambda), \quad (10)$$

$$PL = 20\lg\left(\frac{4\pi r}{\lambda}\right) - PF, \quad (11)$$

where λ is the wavelength and r is the range of the radio wave propagation.

RAY TRACING METHOD BASED ON THE ORDINARY DIFFERENTIAL EQUATION OF THE 2ND ORDER

This section describes an algorithm for ray tracing in tropospheric layers. It calculates the number of beams and their azimuthal and angular coordinates in the antenna array opening with subsequent digital processing. We write Snell's law (1) by rewriting h as a function of r, that is:

$$n\left[h(r)\right]\left[R_\mathrm{E} + h(r)\right]\cos e = \mathrm{const}. \quad (12)$$

For infinitesimal dh and dr, the geometric representation of the quantities (Fig. 2) gives the following [18]:

$$\sin e = \frac{dh}{dr}, \quad (13)$$

$$\cos e = \sqrt{1-\left(\frac{dh}{dr}\right)^2}\left(\geq 0, \text{ т.е. } e \in \left[-\frac{\pi}{2}, \frac{\pi}{2}\right]\right). \quad (14)$$

Then,

$$nh(r)\left[R_\mathrm{E} + h(r)\right]\sqrt{1-\left(\frac{dh}{dr}\right)^2} = \mathrm{const}. \quad (15)$$

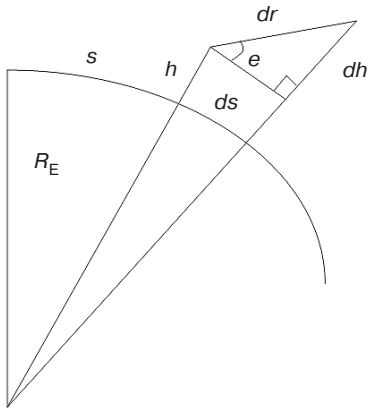

Fig. 2. Geometric representation of R_E, h, and s and their differentials

Assuming h is a function of r, refractive index n implicitly depends on r. Differentiating Eq. (15) with respect to r gives the following:

$$\frac{dn}{dh}\frac{dh}{dr}\left(R_\mathrm{E}+h\right)\sqrt{1-\left(\frac{dh}{dr}\right)^2} + n\frac{dh}{dr}\sqrt{1-\left(\frac{dh}{dr}\right)^2} + n\left(R_\mathrm{E}+1\right)\frac{-2\frac{dh}{dr}\frac{d^2h}{dr^2}}{2\sqrt{1-\left(\frac{dh}{dr}\right)^2}} = 0. \quad (16)$$

The equivalent system of two coupled equations of the first order is obtained after simple transformations and the introduction of the substitution $\frac{dh}{dr} = u$, as follows [18]:

$$\frac{dh}{dr} = u, \quad (17)$$

[5] Ehn J. *Propagation of Radio Waves in a Realistic Environment using a Parabolic Equation Approach*. PhD Thesis. 2019. https://urn.kb.se/resolve?urn=urn:nbn:se:liu:diva-157610. Accessed October 09, 2023.

$$\frac{du}{dr} = -u^2\left(\frac{1}{n}\frac{dn}{dh} + \frac{1}{R_E + h}\right) + \left(\frac{1}{n}\frac{dn}{dh} + \frac{1}{R_E + h}\right). \quad (18)$$

Equations (17) and (18) can be considered as an initial value problem:

$$u(r=0) = \left.\frac{dh}{dr}\right|_{r=0} = \sin e_0, \quad (19)$$

$$h(r=0) = h_0. \quad (20)$$

This ordinary differential equation uniquely solves the ray tracing problem.

Equations (17) and (18) are discretized and solved in iteration steps of Δr. The value of the iteration step from $(l-1)$ to l is determined as follows [18].

Step 1: Estimate the values $\frac{1}{n_{l-1}}$ and $\left.\frac{dn}{dh}\right|_{l-1}$ at height h_{l-1} using experimental data or approximations.

Step 2. Solve Eqs. (17) and (18) with the initial values u_{l-1} and h_{l-1} to obtain the values u_l and h_l.

Step 3. Calculate s_l, which is the propagation distance of the beam at the step l, as follows:

$$s_l = s_{l-1} + R_E \arcsin\left(\frac{\cos e_{l-1}\Delta r}{R_E + h_l}\right), \quad (21)$$

and the angle

$$e_l = \arcsin(u_{l-1}). \quad (22)$$

Steps 1–3 are repeated from $l = 1$ to $l = L$, which corresponds to the endpoint of the calculation of the beam propagation paths. The numerical differentiation in step 2 is carried out using the 4th order Runge–Kutta method. For the first iteration, $l = 1$, the initial values in step 2 are given by Eqs. (19) and (20). The refractive index and its derivative should be evaluated at the height h_0 where the transmitting antenna is located, giving the values $\frac{1}{n_0}$ and $\left.\frac{dn}{dh}\right|_0$, respectively. The distance from the transmitting point to the DAA is thus divided into L points. At each point of l iterations, s_l, e_l, n_l, and h_l are calculated for each beam.

SIMULATION

In the theoretical part of the paper, the methods for calculating the propagation of electromagnetic beams in the stratified atmosphere have been presented. The radio signals obtained in this way are combined in the opening of the DAA for subsequent spatial filtering, the scheme of which is shown in Fig. 3 [19].

Consider an antenna array consisting of K directional antenna elements (AEs). It receives D independent signals from different directions with azimuth θ_D and location angle ϕ_D as shown in Fig. 3. Here, $q_D(t)$ is the incident signal, while $v_K(t)$ is the received signal from the Kth AE at a discrete time t. In the following, the index "1" denotes the useful signal. Consequently, the DAA output signal matrix has the following form:

$$\vec{\mathbf{v}} = \mathbf{A}\vec{\mathbf{q}} + \vec{\mathbf{n}}, \quad (23)$$

where $\vec{\mathbf{n}}$ is the noise vector; $\mathbf{A}$ is the matrix of scan vectors $\vec{\mathbf{a}}(\theta, \phi)$ determining the array field amplitude-phase distribution.

Thus,

$$\mathbf{A} = \left[\vec{\mathbf{a}}(\theta_1, \phi_1)\ \ \vec{\mathbf{a}}(\theta_2, \phi_2) \cdots \vec{\mathbf{a}}(\theta_D, \phi_D)\right], \quad (24)$$

$$\vec{\mathbf{a}}(\theta, \phi) = \left[g_1(\theta, \phi)e^{j\mathbf{k}\mathbf{r}_1^T} \quad g_2(\theta, \phi)e^{j\mathbf{k}\mathbf{r}_2^T} \quad \ldots \quad g_K(\theta, \phi)e^{j\mathbf{k}\mathbf{r}_K^T}\right], \quad (25)$$

where $\mathbf{k} = \frac{2\pi}{\lambda}(k_x, k_y, k_z) = \frac{2\pi}{\lambda}(\sin\phi\cos\theta, \sin\phi\sin\theta, \cos\phi)$ is the wave vector; $\mathbf{r}_n^T = (x_n, y_n, z_n)^T$ is the radius

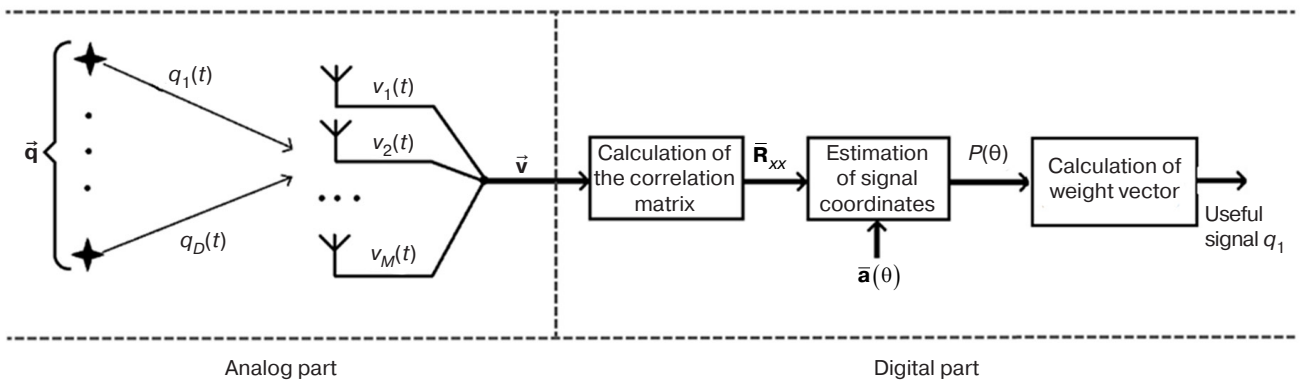

Fig. 3. Scheme of signal processing in DAA

vector to the nth AE; $g_n(\theta, \phi)$ is the array pattern of the nth AE.

The following equation determines the spatial correlation matrix of the signals:

$$\hat{\mathbf{R}} = \frac{1}{T}\sum_{t=1}^{T}\vec{\mathbf{v}}(t)^{\mathrm{H}}\vec{\mathbf{v}}(t), \quad (26)$$

where T is the number of samples of the digital signal, while the index H indicates the Hermite transpose of the vector $\vec{\mathbf{v}}(t)$.

The angular coordinates of the signals are then determined using the multiple signal classification (MUSIC) method[6], which is essentially structural and overcomes the Rayleigh criterion resolution. This means that its resolution is less than the main lobe width of the array pattern [20]:

$$P_{\mathrm{MU}}(\theta) = \frac{1}{\left|\vec{\mathbf{a}}^{\mathrm{H}}(\theta)\mathbf{E}_{\mathrm{noise}}\mathbf{E}_{\mathrm{noise}}^{\mathrm{H}}\vec{\mathbf{a}}(\theta)\right|}, \quad (27)$$

where $\mathbf{E}_{\mathrm{noise}}$ is the noise eigenvector.

The weighting factor vector for the formation of the DAA array pattern is calculated as follows [21]:

$$\vec{\mathbf{w}} = \frac{\mathbf{R}^{-1}\vec{\mathbf{a}}(\theta_1, \phi_1)}{\vec{\mathbf{a}}(\theta_1, \phi_1)^{\mathrm{H}}\mathbf{R}^{-1}\vec{\mathbf{a}}(\theta_1, \phi_1)}. \quad (28)$$

Thus, the DAA determines the spatial coordinates of the signal in accordance with Eqs. (26) and (27) to form the array pattern in the digital domain on the basis of the obtained vector $\vec{\mathbf{w}}$. Then the signal at the output is as follows:

$$q_1 = \vec{\mathbf{w}}\vec{\mathbf{v}}. \quad (29)$$

On the basis of simulation, a study was carried out to estimate the propagation range of telecommunication signals in the tropospheric layers. In all cases, the maximum range is chosen to be equal to 150 km with a resolution Δr equal to 500 m. Obviously, the tracking of all the rays from a transmitter arriving at the receiving DAA would require ray tracing over the full range of declination angles. However, the expression giving the limits of the declination angle within which radio wave propagation occurs in an airborne tropospheric waveguide is well known [22]:

$$\varphi_{\min,\max} = \pm\sqrt{2\left(\frac{1}{n(0)}\frac{dn}{dh} - \frac{1}{R_0}\right)(h_t - \delta)}, \quad (30)$$

[6] Multiple signal classification is an algorithm for estimating sinusoidal sum frequencies against noise from a series of measurements and for determining angular coordinates of multiple signal sources in digital antenna arrays.

where δ is the trapping layer thickness and h_t is the transmitting antenna height.

The generalized scheme of the simulation is shown in Fig. 4. In the experiments, the transmitter antenna is mounted at a height of 200 m under noise and multipath conditions. The signal used is a 1 Mbit/s binary phase-shift keyed signal. The transmitter power is 10 W, while the noise power in the ultrashort wavelength range is $1.7 \cdot 10^{-13}$ W [23]. The bit error rate is estimated as the ratio of the number of bits received in error to the total number of bits.

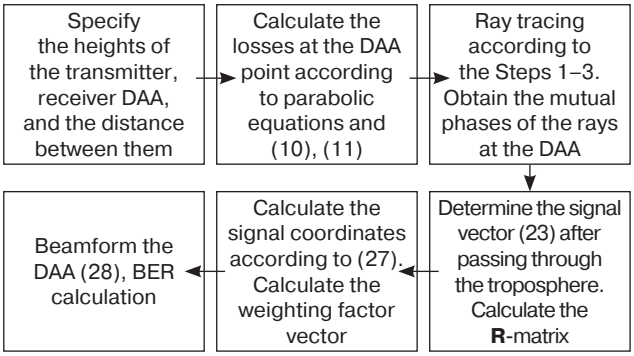

Fig. 4. Generalized scheme of simulation

Experiment 1: Idealized surface tropospheric waveguide

In this experiment, a surface waveguide is simulated. The modified refractive profile is shown in Fig. 5. It has a negative slope of −100 M-units km^{-1} in the height range from 0 to 350 m and a slope of 117 M-units km^{-1}.

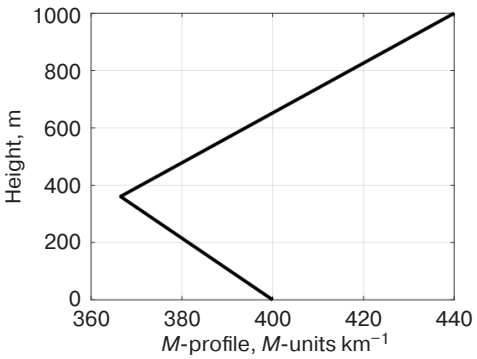

Fig. 5. Modified M-profile of the surface waveguide

The electromagnetic field distribution as a function of the distance from the transmitter and height above the Earth's surface is shown in Fig. 6. The calculation is made using the PU apparatus and the numerical Fourier splitting algorithm. The carrier frequency is 5 GHz, while the transmitter antenna is a half-wave dipole.

Figure 6 shows that the field distribution is not uniform.

The rays for the refractive profile considered are shown in Fig. 7.

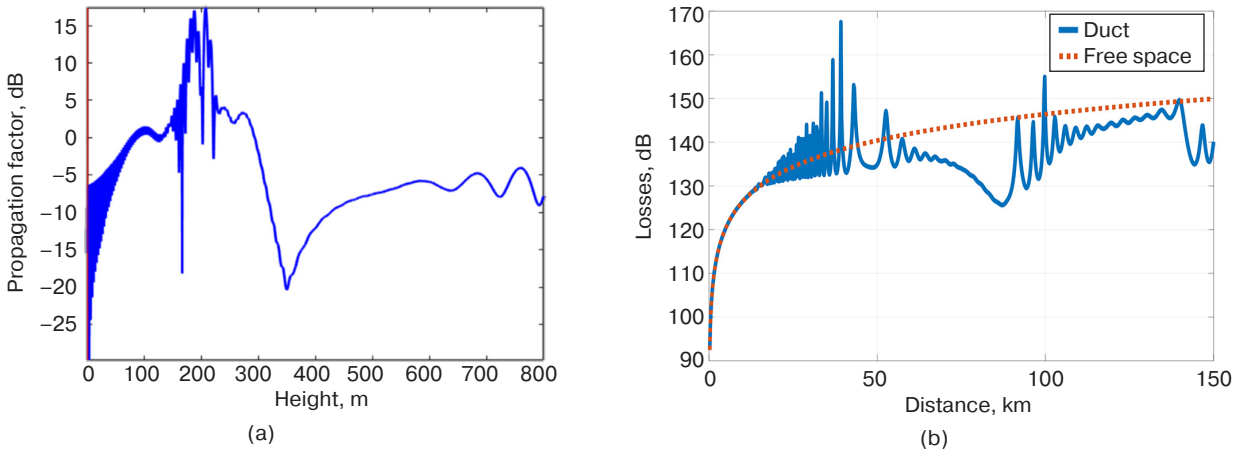

Fig. 6. Field distribution parameters:
(a) propagation factor for a vertical slice at a height of 25 km,
(b) losses in a horizontal slice at a height of 200 m (the solid blue line is in the atmosphere presented in Fig. 5; the dotted red line is in free space)

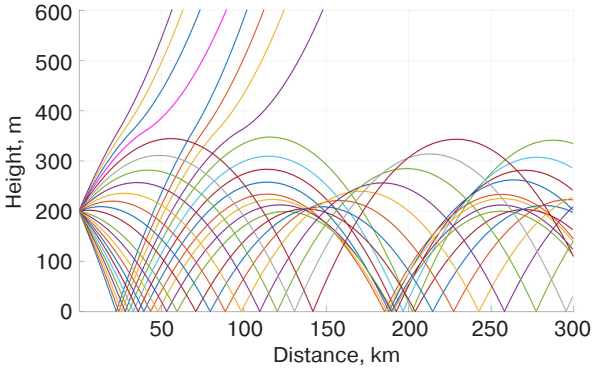

Fig. 7. Rays propagating in the lower layers of the tropospheric waveguide

It can be seen that the rays are reflected from the upper boundary of the trapping layer. They then reach the Earth's surface where they are reflected again. This process continues up to the receiver DAA, which is attenuated as shown in Fig. 6. One of these rays crossing the receiving DAA is shown in Fig. 8.

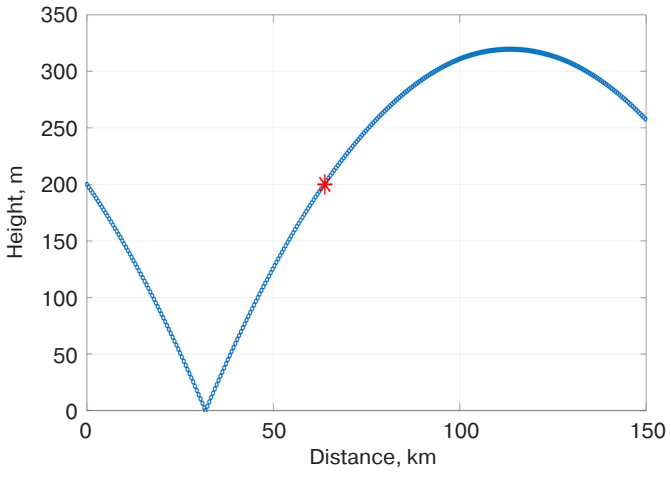

Fig. 8. Example of ray crossing (blue line) and DAA (red asterisk)

The graph showing the BER depending on the type of antenna array used and the distance over which reception could be achieved (50 to 100 km from the transmitter) is shown in Fig. 9. The radio signal attenuation is approximately −135 dB in this case. The circular and the hemispherical geometry of the receiving DAAs with directional AEs are used [23].

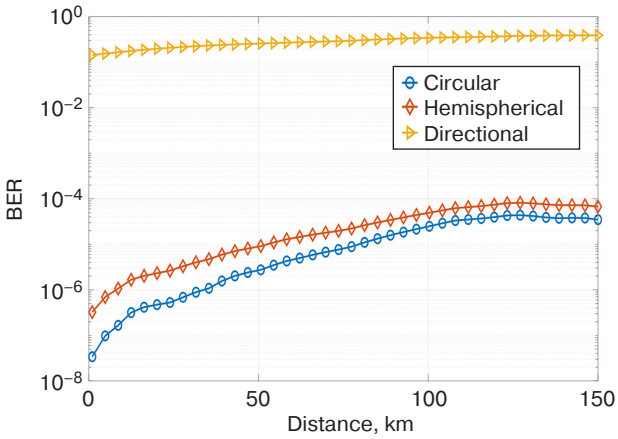

Fig. 9. BER vs distance

The graphs in Fig. 9 show that the circular DAA provides the lowest BER (up to 10^{-6}) at distances up to 50 km. If a hemispherical shape of the receiving DAA is used with a directional antenna, the BER value at this distance is about 10^{-5} and 0.3, respectively. This is in agreement with previous results [19]. In this case, the attenuation of the signal after passing through the atmosphere is about 135 dB as shown in Fig. 6; then, the ratio of the signal power to the noise power at the output of each receiving AE is 10 dB. Simultaneously, there is no obvious dependence of bit error on distance in Fig. 9 and beyond, especially from 15 km. This can be explained by the fact that, as can be seen from Eq. (11), the value of the power loss is linearly dependent on the

distance travelled by the radio wave, whereas the field strength is inversely proportional to $\sqrt{r}$.

Experiment 2: Idealized S-shaped tropospheric waveguide

Consider an idealized S-shaped channel surface characterized by the M and N profiles as shown in Fig. 10. The M profile starts with a slope of 117 M-units km^{-1} for the lowest 100 m and then changes to a slope of −100 M-units km^{-1} up to a height of 400 m, after which it returns to the value of 117 M-units km^{-1}.

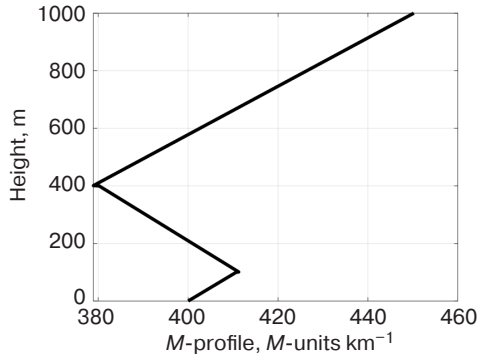

Fig. 10. Modified M-profile of atmospheric layers

The characteristics of the electromagnetic field distribution according to the profile of the modified refractive index shown in Fig. 10 are shown in Fig. 11.

It can be seen from Fig. 11a that the PF at the transmitter height of 200 m is 15 dB higher than that of the wave in free space. Loss values as a function of the distance between the transmitter and the receiving DAA are plotted in Fig. 11b. From this it can be concluded that the electromagnetic wave inside the tropospheric waveguide loses 15–20 dB less power than the radio signal in free space or outside the trapping layer.

The ray trajectories for the type of refractive index under consideration are shown in Fig. 12.

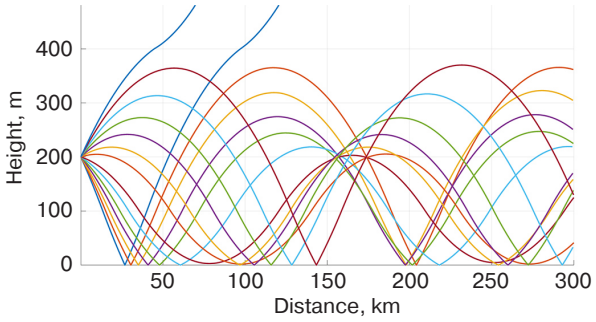

Fig. 12. Rays propagating in the lower layers of the tropospheric waveguide

It can be seen that the rays can be both reflected back from the Earth's surface and refracted at the lower and upper boundaries of the tropospheric layers.

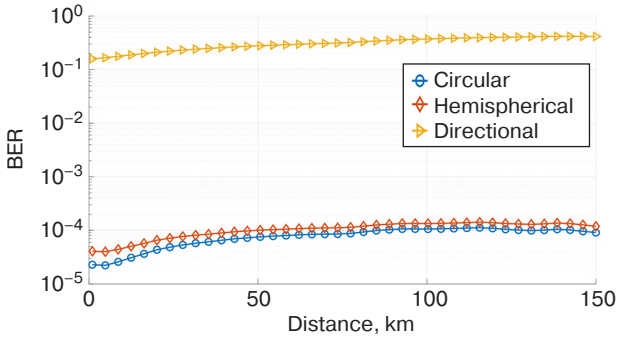

Fig. 13. BER vs distance

The circular DAA gives the lowest BER as shown in Fig. 13. From the analysis of Fig. 11–13, it can be concluded that radio signals at a frequency of 5 GHz can reach a receiver located more than 100 km from the transmitter with BER within 10^{-5}, which is acceptable for the majority of modern wireless telecommunications systems.

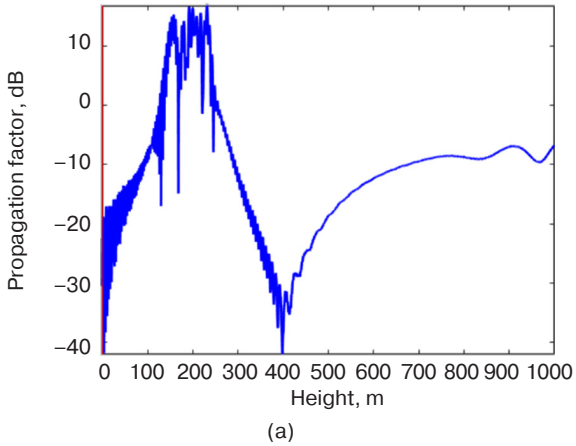

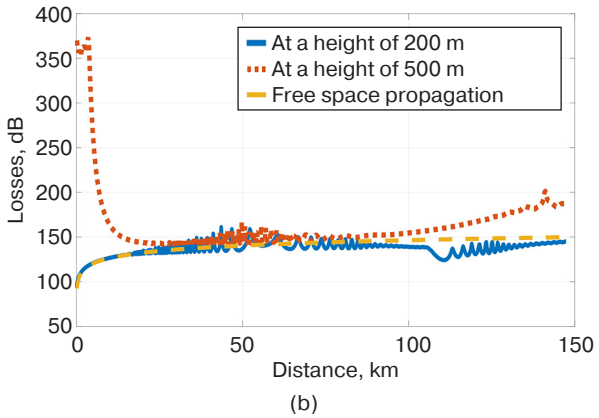

Fig. 11. Field distribution characteristics:
(a) propagation factor for the vertical slice at 110 km,
(b) losses for the horizontal slice

Experiment 3. Ideal elevated waveguide

Consider an ideal elevated waveguide, whose corresponding *M*-profile is shown in Fig. 14. The modified *M*-profile starts with a slope of 117 *M*-units km^{-1} for the first 250 m of height. It then changes to −100 *M*-units km^{-1} up to 400 m before returning to 117 *M*-units km^{-1}. Within the trapping layer, the antenna height is 300 m.

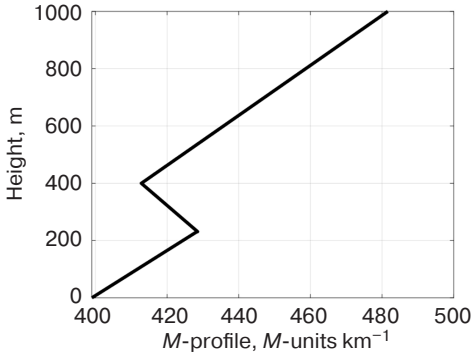

Fig. 14. Modified *M*-profile typical of an elevated waveguide

It can be seen from Fig. 14 that the waveguide in this case is elevated and does not touch the Earth's surface. Figure 15 depicts the distribution of the electromagnetic field as a function of the distance from the transmitter and the height above the Earth's surface.

As shown in Fig. 15a, the 5 GHz electromagnetic wave at a transmitting height of 300 m has a higher power compared to free rectilinear propagation. It is also clear from Fig. 15b that the advantage of propagation inside the tropospheric waveguide becomes apparent at distances above 100 km, where the loss is 20 dB less than in free space.

Typical ray trajectories for an elevated waveguide are shown in Fig. 16.

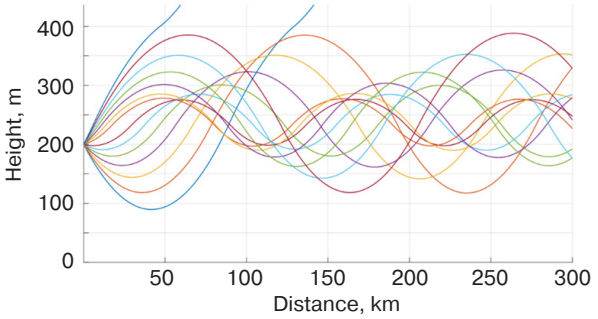

Fig. 16. Rays propagating in the lower layers of a tropospheric waveguide

In this case, it is clear that the rays, which are only refracted at the upper and lower limits of the refractive index variation, do not reach the Earth's surface.

The graphs of BER versus distance between transmitter and DAA inside the waveguide, also at 300 m height, are shown in Fig. 17.

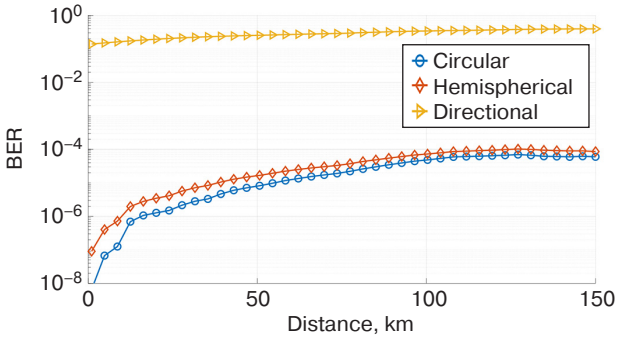

Fig. 17. BER vs distance

The graphs in Fig. 17 show that the circular DAA gives the lowest BER (10^{-6}) compared to the hemispherical geometry and simple directional antenna up to 50 km, where the BER is 10^{-5} and 0.3, respectively. This geometry offers the advantage that

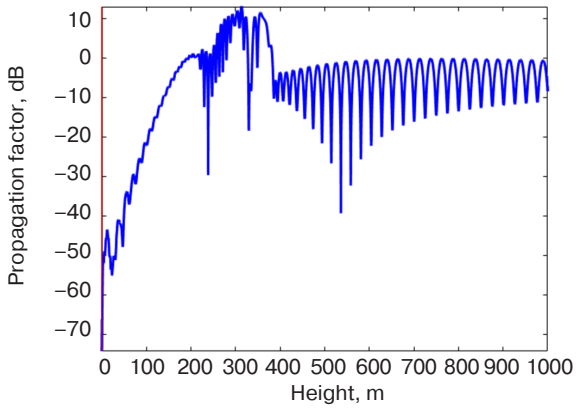

(a)

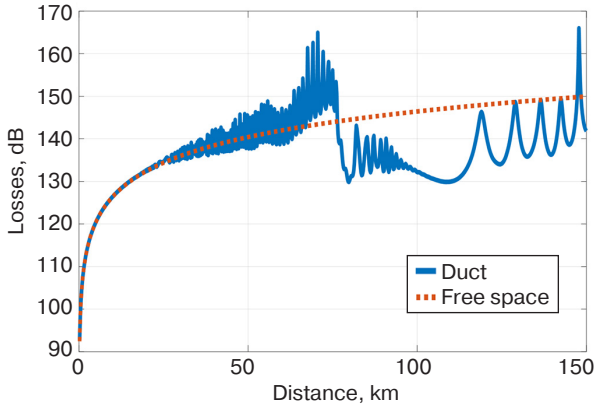

(b)

Fig. 15. Field distribution parameters:
(a) propagation factor for a vertical slice at 80 km,
(b) losses in a horizontal slice at a height of 50 m (the solid blue line is in the atmosphere shown in Fig. 2; the dotted red line is in free space)

the electromagnetic rays reaching the array inside the tropospheric waveguide have negligible declination angles, most of them being $\varphi \approx 90°$.

CONCLUSIONS

When a modified refractive index changes from a maximum near the Earth's surface to a minimum at a certain altitude, a tropospheric waveguide manifests in the lower atmosphere. In this case, the electromagnetic radiation in the ultrashort centimeter-wave range (5 GHz) from the transmitter does not propagate in a straight line, but instead propagates by reflection from the Earth (or the lower trapping layer) and refraction from the upper trapping layer. Stable receiving distances are limited to several hundred kilometers, resulting in significant attenuation. In addition, a number of rays with different amplitudes and phases may be present at the receiving point, resulting in multipath propagation. In order to overcome such difficulties, the use of antenna arrays with digital formation of the array pattern on the receiver side is proposed.

The presented approaches for correctly modelling signal propagation in the tropospheric waveguide and DAA include the calculation of propagation paths and losses taking into account distance, refractive index, antenna height, and carrier frequency. The rays appearing in the opening of the DAA antenna are obtained. In the final stage, the BER is estimated by evaluating the angular coordinates of the rays and the digital beamforming procedure.

When combined with digital spatial processing, a circular antenna array shape is shown to be optimal.

ACKNOWLEDGMENTS

The study was supported by the Russian Science Foundation, project No. 23-21-00125, https://rscf.ru/project/23-21-00125/.

Authors' contributions

I.W. Peshkov—setting the goals and objectives of the study, development of processing methods, conducting research.

D.N. Borisov—research planning, scientific editing of the article, interpretation and generalization of the results.

REFERENCES

1. Schelleng J.C., Burrows C.R., Ferell E.B. Ultra-shortwave propagation. In: *Proceedings of the Institute of Radio Engineers* (*Proc. I.R.E.*). 1933;21(3):427–463. https://doi.org/10.1109/JRPROC.1933.227639
2. Anderson K. Radar measurements at 16.5 GHz in the oceanic evaporation duct. *IEEE Trans. Antennas Propag.* 1989;37(1):100–106. https://doi.org/10.1109/8.192171
3. Ivanov V.K., Shalyapin V.N., Levadny Y.V. Microwave scattering by tropospheric fluctuations in an evaporation duct. *Radiophys. Quantum. El.* 2009;52(4):277–286. https://doi.org/10.1007/s11141-009-9133-z
[Original Russian Text: Ivanov V.K., Shalyapin V.N., Levadny Y.V. Microwave scattering by tropospheric fluctuations in an evaporation duct. *Izvestiya Vysshikh Uchebnykh Zavedenii. Radiofizika.* 2009;52(4):307–317 (in Russ.).]
4. Dinc E., Akan O.B. Beyond-line-of-sight communications with ducting layer. *IEEE Commun. Mag*. 2014;52(10):37–43. https://doi.org/10.1109/MCOM.2014.6917399
5. Ma J., Wang J., Yang C. Long-Range Microwave Links Guided by Evaporation Ducts. *IEEE Commun. Mag.* 2022;60(5):68–72. https://doi.org/10.1109/MCOM.002.00508
6. Woods G.S., Ruxton A., Huddlestone-Holmes C., Gigan G. High-Capacity, Long-Range, Over Ocean Microwave Link Using the Evaporation Duct. *IEEE J. Oceanic Eng*. 2009;34(3):323–330. https://doi.org/10.1109/JOE.2009.2020851
7. Mentes Ş., Kaymaz Z. Investigation of Surface Duct Conditions over Istanbul, Turkey. *J. Appl. Meteor. Climatol*. 2007;46(3):318–337. https://doi.org/10.1175/JAM2452.1
8. Pishchin O.N., Kalambatskaya O.V. Characteristics of UHF waves distribution in land and water surface tropospheric waveguide. *Vestnik Astrakhanskogo gosudarstvennogo tekhnicheskogo universiteta. Seriya: Upravlenie, vychislitel'naya tekhnika i informatika = Vestnik of Astrakhan State Technical University. Series: Management, Computer Science and Informatics.* 2019;4:115–121 (in Russ.). https://doi.org/10.24143/2072-9502-2019-4-115-121
9. Pishchin O.N. The analysis and experimental researches of attenuation of a radio signal of systems of a cellular mobile radio communication above a water smooth surface. *Izvestiya Yuzhnogo federal'nogo universiteta. Seriya: Tekhnicheskie nauki* (*Izvestiya YuFU. Seriya: tekhnicheskie nauki*) = *Izvestiya SFedU. Engineering Sciences*. 2009;1:43–49 (in Russ.).
10. Hartree D.R., Michel J.G.L., Nicolson P. Practical methods for the solution of the equations of tropospheric refraction. In: *Meteorological Factors in Radio-Wave Propagation. Report of a Conference. The Physical Society and The Royal Meteorological Society*. 1947. P. 127–168.
11. Dedov N.M., Tolstykh V.D., Serebryakov M.A. The influence of tropospheric ducts on the radar operation over the sea surface. In: *Actual Problems of the Activities of Departments of the Penal System: Collection of Materials of the All-Russian Scientific and Practical Conference*: in 2 v. Voronezh; 2020. P. 128–132 (in Russ.). https://www.elibrary.ru/nptlot
12. Leontovich M.A., Fok V.A. Solution of propagation of electromagnetic waves along the Earth's surface by the method of parabolic equations. *J. Phys. USSR.* 1946;10(1):13–23.

13. Akhiyarov V.V. Attenuation factor calculation for backscattering from the terrain using the parabolic equation technique. *Zhurnal radioelektroniki = J. Radio Electronics*. 2019;11 (in Russ.). https://doi.org/10.30898/1684-1719.2019.11.1
14. Zhang P., Lu Bai, Wu Z., Guo L. Applying the parabolic equation to tropospheric groundwave propagation: A review of recent achievements and significant milestones. *IEEE Trans. Antennas Propag. Mag*. 2016;58(3):31–44. https://doi.org/10.1109/MAP.2016.2541620
15. Levy M. *Parabolic Equation Methods for Electromagnetic Wave Propagation*. London: IET; 2000. 336 p.
16. Ozlem O., Gokhan A., Mustafa K., Levent S. PETOOL: MATLAB-based one-way and two-way split-step parabolic equation tool for radiowave propagation over variable terrain. *Computer Phys. Commun*. 2011;182(12):2638–2654. https://doi.org/10.1016/j.cpc.2011.07.017
17. Sirkova I. Propagation Factor and Path Loss Simulation Results for Two Rough Surface Reflection Coefficients Applied to the Microwave Ducting Propagation Over the Sea. *Progress In Electromagnetics Research M.* (*PIERM*). 2011;17:151–166. http://doi.org/10.2528/PIERM11020602
18. Zeng Y., Blahak U., Neuper M., Jerger D. Radar Beam Tracing Methods Based on Atmospheric Refractive Index. *J. Atmos. Oceanic Technol*. 2014;31(12):2650–2670. https://doi.org/10.1175/JTECH-D-13-00152.1
19. Nechaev Y.B., Peshkov I.V. Study of digital diagram formation for optimum interference and noise reduction in antenna arrays of different shapes with directional radiators. *Fizika volnovykh protsessov i radiotekhnicheskie sistemy = Physics of Wave Processes and Radio Systems*. 2022;25(2):73–82 (in Russ.). https://doi.org/10.18469/1810-3189.2022.25.2.73-82
20. Schmidt R.O Multiple Emitter Location and Signal Parameter Estimation. *IEEE Trans. Antennas Propag*. 1986;AP-34(3):276–280. https://doi.org/10.1109/TAP.1986.1143830
21. Balanis C., Ioannides P. *Introduction to Smart Antennas*. San Rafael: Morgan & Claypool Publishers; 2007. 174 p.
22. Dinc E., Akan O.B. Channel Model for the Surface Ducts: Large-Scale Path-Loss, Delay Spread, and AOA. *IEEE Trans. Antennas and Propag.* 2015;63(6):2728–2738. http://doi.org/10.1109/TAP.2015.2418788
23. Nechaev Y.B., Peshkov I.W. Simulation of Digital and Analog Spatial Filtering of VHF Signals in Channel with Losses due to Multipple Diffraction. In: *2022 Systems of Signals Generating and Processing in the Field of on Board Communications*. 2022. https://doi.org/10.1109/IEEECONF53456.2022.9744371

СПИСОК ЛИТЕРАТУРЫ

1. Schelleng J.C., Burrows C.R., Ferell E.B. Ultra-shortwave propagation. In: *Proceedings of the Institute of Radio Engineers* (*Proc. I.R.E.*). 1933;21(3):427–463. https://doi.org/10.1109/JRPROC.1933.227639
2. Anderson K. Radar measurements at 16.5 GHz in the oceanic evaporation duct. *IEEE Trans. Antennas Propag.* 1989;37(1):100–106. https://doi.org/10.1109/8.192171
3. Иванов В.К., Шаляпин В.Н., Левадный Ю.В. Рассеяние ультракоротких радиоволн на тропосферных флуктуациях в приводном волноводе. *Известия вузов. Радиофизика.* 2009;52(4):307–317.
4. Dinc E., Akan O.B. Beyond-line-of-sight communications with ducting layer. *IEEE Commun. Mag*. 2014;52(10):37–43. https://doi.org/10.1109/MCOM.2014.6917399
5. Ma J., Wang J., Yang C. Long-Range Microwave Links Guided by Evaporation Ducts. *IEEE Commun. Mag.* 2022;60(5):68–72. https://doi.org/10.1109/MCOM.002.00508
6. Woods G.S., Ruxton A., Huddlestone-Holmes C., Gigan G. High-Capacity, Long-Range, Over Ocean Microwave Link Using the Evaporation Duct. *IEEE J. Oceanic Eng*. 2009;34(3):323–330. https://doi.org/10.1109/JOE.2009.2020851
7. Mentes Ş., Kaymaz Z. Investigation of Surface Duct Conditions over Istanbul, Turkey. *J. Appl. Meteor. Climatol*. 2007;46(3):318–337. https://doi.org/10.1175/JAM2452.1
8. Пищин О.Н., Каламбацкая О.В. Особенности распространения радиоволн УВЧ диапазона в приземном и приводном тропосферном волноводе. *Вестник Астраханского государственного технического университета. Серия: Управление, вычислительная техника и информатика*. 2019;4:115–121. https://doi.org/10.24143/2072-9502-2019-4-115-121
9. Пищин О.Н. Анализ и экспериментальные исследования затухания радиосигнала систем сотовой подвижной радиосвязи над водной гладью. *Известия ЮФУ. Серия: Технические науки*. 2009;1:43–49.
10. Hartree D.R., Michel J.G.L., Nicolson P. Practical methods for the solution of the equations of tropospheric refraction. In: *Meteorological Factors in Radio-Wave Propagation. Report of a Conference. The Physical Society and The Royal Meteorological Society*. 1947. P. 127–168.
11. Дедов Н.М., Толстых В.Д., Серебряков М.А. Влияние тропосферных волноводов на работу радиолокатора над морской поверхностью. В сб.: *Актуальные проблемы деятельности подразделений уголовно-исполнительной системы:* Сборник материалов Всероссийской научно-практической конференции в 2-х т. Воронеж; 2020. Т. 1. С. 128–132. https://www.elibrary.ru/nptlot
12. Leontovich M.A., Fok V.A. Solution of propagation of electromagnetic waves along the Earth's surface by the method of parabolic equations. *J. Phys. USSR.* 1946;10(1):13–23.
13. Ахияров В.В. Вычисление множителя ослабления при обратном рассеянии от земной поверхности методом параболического уравнения. *Журнал радиоэлектроники*. 2019;11. https://doi.org/10.30898/1684-1719.2019.11.1
14. Zhang P., Lu Bai, Wu Z., Guo L. Applying the parabolic equation to tropospheric groundwave propagation: A review of recent achievements and significant milestones. *IEEE Trans. Antennas Propag. Mag*. 2016;58(3):31–44. https://doi.org/10.1109/MAP.2016.2541620

15. Levy M. *Parabolic Equation Methods for Electromagnetic Wave Propagation*. London: IET; 2000. 336 p.
16. Ozlem O., Gokhan A., Mustafa K., Levent S. PETOOL: MATLAB-based one-way and two-way split-step parabolic equation tool for radiowave propagation over variable terrain. *Computer Phys. Commun*. 2011;182(12):2638–2654. https://doi.org/10.1016/j.cpc.2011.07.017
17. Sirkova I. Propagation Factor and Path Loss Simulation Results for Two Rough Surface Reflection Coefficients Applied to the Microwave Ducting Propagation Over the Sea. *Progress In Electromagnetics Research M.* (*PIERM*). 2011;17:151–166. http://doi.org/10.2528/PIERM11020602
18. Zeng Y., Blahak U., Neuper M., Jerger D. Radar Beam Tracing Methods Based on Atmospheric Refractive Index. *J. Atmos. Oceanic Technol*. 2014;31(12):2650–2670. https://doi.org/10.1175/JTECH-D-13-00152.1
19. Нечаев Ю.Б., Пешков И.В. Исследование цифрового диаграммообразования для оптимального помехо- и шумоподавления в антенных решетках различной формы с направленными излучателями. *Физика волновых процессов и радиотехнические системы*. 2022;25(2):73–82. https://doi.org/10.18469/1810-3189.2022.25.2.73-82
20. Schmidt R.O Multiple Emitter Location and Signal Parameter Estimation. *IEEE Trans. Antennas Propag*. 1986;AP-34(3): 276–280. https://doi.org/10.1109/TAP.1986.1143830
21. Balanis C., Ioannides P. *Introduction to Smart Antennas*. San Rafael: Morgan & Claypool Publishers; 2007. 174 p.
22. Dinc E., Akan O.B. Channel Model for the Surface Ducts: Large-Scale Path-Loss, Delay Spread, and AOA. *IEEE Trans. Antennas and Propag.* 2015;63(6):2728–2738. http://doi.org/10.1109/TAP.2015.2418788
23. Nechaev Y.B., Peshkov I.W. Simulation of Digital and Analog Spatial Filtering of VHF Signals in Channel with Losses due to Multipple Diffraction. In: *2022 Systems of Signals Generating and Processing in the Field of on Board Communications*. 2022. https://doi.org/10.1109/IEEECONF53456.2022.9744371

About the authors

Ilia W. Peshkov, Cand. Sci. (Phys.–Math.), Associate Professor, Department of Physics, Radio Engineering and Electronics, Bunin Yelets State University (28, Kommunarov ul., Yelets, 399770 Russia). E-mail: ilvpeshkov@gmail.com. Scopus Author ID 7003332128, ResearcherID L-6734-2013, RSCI SPIN-code 8009-4805, https://orcid.org/0000-0001-8370-6954

Dmitry N. Borisov, Cand. Sci. (Eng.), Associate Professor, Head of the Department of Information systems, Voronezh State University (1, Universitetskaya pl., Voronezh, 394018 Russia). E-mail: borisov@sc.vsu.ru. Scopus Author ID 54901090900, ResearcherID J-5289-2014, RSCI SPIN-code 6556-0285, https://orcid.org/0000-0002-1265-7195

Об авторах

Пешков Илья Владимирович, к.ф.-м.н., доцент, кафедра физики, радиотехники и электроники, ФГБОУ ВО «Елецкий государственный университет им. И.А. Бунина» (399770, Россия, Елец, ул. Коммунаров, д. 28). E-mail: ilvpeshkov@gmail.com. Scopus Author ID 7003332128, ResearcherID L-6734-2013, SPIN-код РИНЦ 8009-4805, https://orcid.org/0000-0001-8370-6954

Борисов Дмитрий Николаевич, к.т.н. доцент, заведующий кафедрой информационных систем, ФГБОУ ВО «Воронежский государственный университет» (394018, Россия, Воронеж, Университетская пл., д. 1). E-mail: borisov@sc.vsu.ru. Scopus Author ID 54901090900, ResearcherID J-5289-2014, SPIN-код РИНЦ 6556-0285, https://orcid.org/0000-0002-1265-7195

Translated from Russian into English by K. Nazarov
Edited for English language and spelling by Thomas A. Beavitt